

Journal of Materials Chemistry B

Accepted Manuscript



This is an *Accepted Manuscript*, which has been through the Royal Society of Chemistry peer review process and has been accepted for publication.

Accepted Manuscripts are published online shortly after acceptance, before technical editing, formatting and proof reading. Using this free service, authors can make their results available to the community, in citable form, before we publish the edited article. We will replace this *Accepted Manuscript* with the edited and formatted *Advance Article* as soon as it is available.

You can find more information about *Accepted Manuscripts* in the [Information for Authors](#).

Please note that technical editing may introduce minor changes to the text and/or graphics, which may alter content. The journal's standard [Terms & Conditions](#) and the [Ethical guidelines](#) still apply. In no event shall the Royal Society of Chemistry be held responsible for any errors or omissions in this *Accepted Manuscript* or any consequences arising from the use of any information it contains.

ARTICLE

Development of redox/pH dual stimuli-responsive MSP@P(MAA-Cy) drug delivery system for programmed release of anticancer drugs in tumour cells

Cite this: DOI: 10.1039/x0xx00000x

Received 00th January 2012,

Accepted 00th January 2012

DOI: 10.1039/x0xx00000x

www.rsc.org/

Dian Li,^a Yuting Zhang,^a Sha Jin,^a Jia Guo,^a Haifeng Gao,^b and Changchun Wang*^a

Intelligent nanomaterials that are able to respond to environmental stimuli for sequential release of multiple payloads are highly desirable in application of drug delivery system. In this study, a core/shell-structured nanocarrier with an acid-dissolvable magnetic supraparticle (MSP) as core and a redox-degradable poly(methylacrylic acid-co-N,N-bis(acryloyl)cystamine) (P(MAA-Cy)) as shell was prepared using the distillation-precipitation polymerization technique, in which the magnetic core and the polymer shell were loaded with different guest molecules. Under a physiological condition similar to the cytoplasm of tumour cells, this MSP@P(MAA-Cy) microsphere showed a sequential degradation profile of the shell and the core. With dyes of fluorescein isothiocyanate (FITC) loaded in the core and rhodamine in the shell, the produced MSP-FITC@P(MAA-Cy)-Rho microspheres were applied in HeLa cell and HEK 293T cell cultures, showing selective degradation of the microspheres in HeLa cells to release the rhodamine and FITC dyes in sequence. When two anticancer drugs, paclitaxel (TXL) and doxorubicin (DOX), were loaded separately into the core and the shell domains of the microspheres, the experimental results showed that the MSP-TXL@P(MAA-Cy)-DOX nanodrug exhibited better inhibitive efficacy than the free drugs under the same dosing level, demonstrating the great potential of this stimuli-sensitive drug delivery system for programmed and stimuli-responsive drug release characteristics.

Introduction

In the current cancer chemotherapy research, how to accurately deliver a drug to tumour tissue remains a big challenge.^{1,2} Traditional clinical chemotherapeutic drugs typically have no specific-tissue affinity and kill both tumour and healthy cells at little difference, which limits their clinical applications due to the systemic toxicity and undesired side effects.³ For this end, targeting delivery of chemotherapeutic drugs using magnetic nanocarriers that can be conveniently manipulated by external magnetic field becomes a subject of great interest.⁴⁻⁷

Many magnetic nanomaterials have been developed with special structures to accommodate the drug storage in the inner space.^{8,9} For instance, hollow magnetic nanoparticles with porous shells have been prepared using thermal-decomposition method, and the hollow chambers could be used to load large amounts of anti-cancer drugs.¹⁰ Recently, solvothermal method represents a robust way to synthesize magnetic supraparticles (MSPs) that have solid,¹¹ hollow^{12,13} and mesoporous structures^{14,15} with high colloidal stability for drug delivery. Although these MSPs can carry drug in their inner space, there is lack of controlled release of the drugs to targeted sites.

Recently, the concept of stimuli-responsiveness is introduced into the drug delivery system, since a programmed responsiveness provides the nanocarrier with the property of controlled release of the loaded drugs towards different signals, which minimizes the undesired drug leaking to normal cells and tissues.¹⁶⁻¹⁸ To date, the most intensive studied stimuli include redox,^{19,20} pH,^{21,22} enzyme,^{23,24} photo-irradiation²⁵ and temperature.²⁶ Since there are obvious differences on the pH and redox environments between the normal and tumour cells in their cytoplasm,^{27,28} studies corresponding to these two stimuli attract great attentions.^{29,30} For instance, acid-cleavable hydrozone bonds have been used to link polymer chains to cisplatin, where the hydrozone bonds can be broken and release the cisplatin at low pH.²² In addition, Zhao et. al. reported a doxorubicin (DOX)-loaded mesoporous silica that immobilized an amino- β -cyclodextrin as the mesopore's gate on the silica surface using a disulfide bond. Cleavage of the amino- β -cyclodextrin in glutathione (GSH) environment opened the pore and released the DOX from the mesoporous silica.²⁹ Our group also reported a degradable poly(methacrylic acid) (PMAA) nanogel carrier for drug delivery, which could be degraded into PMAA oligomers and release the drug in an acidic GSH-rich environment.³⁰ Till now, the integration of

dual responsiveness to both pH and redox into one nanocarrier represents a promising strategy for advanced drug delivery.³¹⁻³³

In addition to the consideration of stimuli-responsiveness, strategies of loading the drugs into the nanocarriers often involve covalent bonds,³⁴ electrostatic interactions^{31,35} and supramolecular interactions.³⁶ Recently, a new demand on multiple-drug loading emerges in cancer chemotherapy, which is expected to greatly enhance the therapeutic effect and overcome the drug-resistant in cells by simultaneously applying several anti-cancer mechanisms^{37,38}. For example, a triblock copolymer poly(ethylene glycol)-b-polylysine-SS-polycaprolactone was used to form micelles and load two drugs of DOX and camptothecin (CPT) simultaneously into the core domain (here, SS representing a disulfide bond as the junction point between the two blocks). The CPT and DOX could be synchronously released in cells and effectively kill cells by inhibiting the cells' propagation in different mechanisms.³⁹ Hydrophobic anticancer drug paclitaxel (TXL) could also be incorporated onto the poly(acrylic acid) (PAA) block in a PEG-b-PAA chain before forming micelles with DOX loaded in the core. This dual-drug system showed good antitumor activity, even to the drug-resistant cancer cells.⁴⁰ However, to the best of our knowledge, all the drugs in a multi-drug delivery system reported so far can release under only one stimulus, while a system with a sequential release of multiple drugs loaded in different domains responding to various environmental stimuli has not been reported.

Herein, we present a new type of magnetic composite microspheres MSP@P(MAA-Cy) (Cy denoted as N, N-bis(acryloyl)cystamine) drug delivery system that contained an acid-dissolvable MSP core and a redox-degradable P(MAA-Cy) shell. Anticancer drugs of TXL and DOX were loaded separately in the core and the shell of the MSP@P(MAA-Cy) nanocarrier, and showed a sequential release profile in an acidic GSH-rich environment. Experimental results of mixing these nanodrugs with HeLa cells showed that the MSP-TXL@P(MAA-Cy)-DOX exhibited better inhibitive efficacy than the free drugs in the same dosing level, indicating a new strategy in the anticancer chemotherapy.

Experimental Section

Materials

Iron(III) chloride hexahydrate ($\text{FeCl}_3 \cdot 6\text{H}_2\text{O}$), ammonium acetate (NH_4OAc), ethylene glycol (EG), ethylene diamine ($\text{NH}_2(\text{CH}_2)_2\text{NH}_2$), 4-dimethylaminopyridine (DMAP), methacrylic acid (MAA), anhydrous ethanol, anhydrous acetonitrile (AN), anhydrous methanol, anhydrous acetone were purchased from Shanghai Chemical Reagents Company and used as received. Poly(γ -glutamic acid) (PGA) was purchased from Dingshunyin Biotechnology Company (China) and used as received. Cystamine dihydrochloride was purchased from Acros Company. Hydrazine ($\text{NH}_2\text{NH}_2 \cdot \text{H}_2\text{O}$) was purchased from Sinopharm Chemical Reagent Corp and used as received. Rhodamine-B, acryloyl chloride, fluorescein isothiocyanate (FITC), glutathione (GSH), Dicyclohexylcarbodiimide (DCC), N-(3-dimethylaminopropyl)-N-ethylcarbodiimide hydrochloride (EDC-HCl) and N-Hydroxysuccinimide (NHS) were purchased from Aladdin (Shanghai, China). 2,2-azobisisobutyronitrile (AIBN) was obtained from Sinopharm Chemical Reagent Company and recrystallized from ethanol. Doxorubicin ($\text{DOX} \cdot \text{HCl}$), in the form of a hydrochloride salt, and paclitaxel (TXL) were obtained from Beijing Huafeng United Technology Company. Dulbecco's modified Eagle's medium (DMEM), fetal bovine serum (FBS), penicillin G, streptomycin, and trypsinase were obtained from GIBCO BRL

(Grand Island, NY). Deionized water was used in all experiments. All other chemicals were available commercially and used without further purifications.

Preparation of magnetic supraparticle (MSP)

MSP was prepared using the solvothermal method. In a typical reaction, 1.35 g (5 mmol) of $\text{FeCl}_3 \cdot 6\text{H}_2\text{O}$ was dissolved in 70 mL of ethylene glycol in a 250 mL flask. After adding 1.0 g of PGA and 3.85 g (0.05 mol) of NH_4OAc , the mixture was stirred vigorously for 1 hour at 160 °C to form a homogeneous brownish solution and then transferred into a Teflon-lined stainless-steel autoclave (100 mL capacity) at 200 °C and for 16 hours. After cooled to room temperature, the black MSPs were washed with ethanol under ultrasonic condition and subsequently separated from the supernatant using magnetic force for five times to remove the adsorbed chemicals.

Preparation of MSP-TXL

TXL was incorporated into MSP by the reaction between the hydroxyl group of TXL and the carboxylic acid group of PGA on MSP. In a typical reaction, 200 mg MSPs dispersed in 100 mL DMF was mixed with 200 mg DCC for activating 1 hr. 50 mg TXL and 20 mg DMAP as catalyst were then added to the mixture and stirred for another 24 hours to produce solid product that was washed five times with ethanol under ultrasonic conditions and lyophilized under vacuum for 3 days.

Preparation of MSP-FITC

The MSPs with surface functionalized FITC was prepared in two steps. First, 200 mg MSPs, 200 mg DCC and 192 mg NHS were dispersed in 100 mL DMF. After added 200 μL ethylene diamine, the mixture solution reacted for 24 hours. After the products were rinsed by ethanol for five times, 100 mL FITC aqueous solution (containing 50 mg FITC) was added for reaction of other 2 hours. The final resultant was rinsed five times with ethanol under ultrasonic conditions to effectively remove excess reagents and then lyophilized under vacuum for 3 days.

Synthesis of MSP@P(MAA-Cy), MSP-TXL@P(MAA-Cy) and MSP-FITC@P(MAA-Cy)

The P(MAA-Cy) shell was coated on the magnetic core using distillation-precipitation copolymerization of MAA with cross-linker Cy in anhydrous acetonitrile.³⁰ In a typical synthesis of MSP@P(MAA-Cy), 50 mg of MSPs dispersed in 40 mL acetonitrile was added into a dried 100 mL single-necked flask under ultrasonication for 10 min. A mixture of 200 mg of monomers (weight ratio of MAA to Cy varied from 200:0, 180:20, 160:40, 140:60 to 120:80) and 5.0 mg AIBN was then added to the flask before the flask was immersed in an oil bath and connected with a Liebig condenser and a receiver. The reaction mixture was heated from ambient temperature to the boiling state within 30 min before distilling out about 20 mL of acetonitrile from the reaction mixture in an hour to stop the reaction. The product was separated using magnet and rinsed with ethanol to remove excess amount of reactants and pure polymer microspheres. The MSP-TXL@P(MAA-Cy) and MSP-FITC@P(MAA-Cy) were prepared using similar methods and all the final products were obtained after lyophilizing under vacuum for 3 days.

Preparation of MSP@P(MAA-Cy)-Rho

Rho-NH₂ was first synthesized by rhodamine-B reacting with hydrazine using a literature method.⁴¹ 10 mg of Rho-NH₂ was added into a mixture containing 20 mg of MSP@P(MAA-Cy), 10 mg of EDC and 9.2 mg of NHS in deionized water after 1-hour activation. The reaction was left for an additional 24 hours before the product was collected using magnet and rinsed with ethanol until the supernatant became clear without the colour of rhodamine.

Synthesis of MSP-FITC@P(MAA-Cy)-Rho and MSP-TXL@P(MAA-Cy)-DOX

Both MSP-FITC@P(MAA-Cy)-Rho and MSP-TXL@P(MAA-Cy)-DOX were prepared in similar procedures based on the electrostatic interaction between the carboxylic acid groups in the shell with the amine groups from Rho-NH₂ or DOX. In a typical procedure, 20 mg of MSP-TXL@P(MAA-Cy) and 8 mg of DOX were dispersed in 20 mL of pH=7.4 phosphate buffer solution and stirred for 24 hours at room temperature. The MSP-TXL@P(MAA-Cy)-DOX microspheres were then separated using magnet and washed for three times with pH=7.4 PBS buffer to remove the adsorbed DOX on the surface before lyophilized under vacuum for 3 days.

Redox and acid triggered disassembly of MSP@P(MAA-Cy)

In a typical procedure, 10 mg of MSP@P(MAA-Cy) was dispersed in 50 mL of Na₃Cit/H₃Cit buffer (0.1 M, pH=7.4 or pH=5.0) solution containing GSH (10 mM or not). The solution was placed in a shaking bed at 37 °C with a rotation speed of 200 rpm. At timed intervals, 3 mL of solution was taken out and the particles were collected and re-dispersed in Deionized water for measurements of the dispersion's transmissivity using UV-vis spectroscopy and the Fe element concentration in the supernatant using the Inductively Coupled Plasma (ICP).

Cell uptake of the core/shell microspheres MSP@P(MAA-Cy)

In the measurement of the shell degradation: HeLa cells and HEK 293T cells were separately incubated with 0.01 mg/mL MSP@P(MAA-Cy)-Rho in a twenty four-well cell culture chamber. At predetermined intervals (3, 6 and 24 hours), the cells were washed with DMEM and PBS three times prior to fluorescence measurement of Rhodamine with excitation at 520 nm. In the measurement of the MSP core degradation: a Fe³⁺-selective fluorescence probe (FP-1)⁴¹ was used to monitor the change of the Fe³⁺ concentrations in the cells. The HeLa cells and HEK 293T cells were separately incubated in φ-15mm thin bottom culture chambers with 0.002 mg/mL MSP@P(MAA-Cy). At timed intervals, the cells were washed with DMEM and PBS three times before stained with 0.01 mM FP-1 for 30 min and 0.001 mg/mL DAPI for 20 min. After washing off all the free FP-1 and the DAPI using DMEM and PBS, the cells were observed under confocal laser scanning microscope (CLSM) 405 nm and 542 nm, respectively.

In vitro cell assay of MSP-FITC@P(MAA-Cy)-Rho

HeLa cells and HEK 293T cells were separately incubated in φ-15mm thin bottom culture chambers with 0.01 mg/mL MSP-FITC@P(MAA-Cy)-Rho. After 48-hour incubation, the cells were washed with DMEM and PBS three times followed by 0.001 mg/mL DAPI stained for 20 min. After the DAPI was removed by PBS

washing, the samples were observed by CLSM with excitation wavelengths of 405 nm, 488 nm and 542 nm.

In vitro cell assay of anti-cancer drugs

In vitro cytotoxicity of MSP@P(MAA-Cy)-DOX, MSP-TXL@P(MAA-Cy), MSP-TXL@P(MAA-Cy)-DOX and free DOX were determined separately on HEK 293T cells and HeLa cells using the CCK8 method.³² Specifically, 100 μL of cells were seeded in a 96-well flat culture plate at a density of 1*10⁴ cells per well and subsequently incubated for 24 hours to allow attachment. Samples with different concentrations (0.01, 0.1, 1.0, 10 μg/mL) of DMEM were then added to each group (three wells) for additional 24-hour incubation. After removing previous nutrient solution, the cells were incubated in 110 μL of DMEM containing 10 μL of CCK-8 solution for 1 h. The absorbance of the suspension was measured at 450 nm on an ELISA reader and the cell viability was calculated by means of the following formula:

$$\text{Cell viability} = \frac{\text{OD}_{450(\text{sample})} - \text{OD}_{450(\text{blank})}}{\text{OD}_{450(\text{control})} - \text{OD}_{450(\text{blank})}} * 100\%$$

Characterization

High-resolution transmission electron microscopy (HRTEM) images were taken on a JEM-2010 (JEOL, Japan) transmission electron microscope at an accelerating voltage of 200 kV. Samples dispersed at an appropriate concentration were cast onto a carbon-coated copper grid. The magnetic properties of the microspheres were carried out on a Model 6000 physical property measurement system (Quantum Design, USA) at 300 K. Powder X-ray diffraction (XRD) patterns were obtained using a X'Pert Pro (Panalytical, Netherlands) diffraction meter with Cu K α radiation at $\alpha=0.154$ nm operating at 40 kV and 40 mA. Fourier transform infrared (FT-IR) spectra of different samples were collected on a Magna-550 (Nicolet, USA) spectrometer using KBr pellets. Thermogravimetric analysis (TGA) data was obtained on a Pyris-1 (Perkin Elmer, USA) thermal analysis system under a flowing nitrogen atmosphere and at a heating rate of 20 °C/min from 100 to 800 °C. Zeta potentials and DLS hydrodynamic sizes were collected on the ZEN 3600 (Malvern, UK) Nano ZS instrument, where the laser wavelength was 633 nm. Ultraviolet-visible (UV-vis) absorption spectra were measured using a UV-3150 (Shimadzu, Japan) ultraviolet-visible spectrophotometer. The confocal laser scanning microscope (CLSM) images were achieved by a P-4010 (Hitachi, Japan) spectrometer. The fluorescence emission spectra were recorded with a RF-5301 PC spectrometer (Shimadzu, Japan).

Results and discussion

Preparation and characterization of MSP@P(MAA-Cy) composite microsphere

Uniform core/shell-structured MSP@P(MAA-Cy) microspheres were prepared using the distillation-precipitation polymerization method. Transmission electron microscopy (TEM) image (Fig. 1a) revealed that the MSP cores had a rough surface with a size of approximately 120 nm. After the generation of PMAA shell cross-linked by 30 wt % of Cy, the produced core/shell microspheres had a size of approximately 280 nm with a smooth surface (Fig. 1b, 1c). Additional characterization using STEM confirmed that the Cy as the cross-linking agent uniformly distributed in the PMAA shell network, since the energy dispersive X-ray (EDX) elemental

mapping results showed that the S element distributed in the whole particle while Fe element concentrated in the core (Fig. 1d-1g). The MSP@P(MAA-Cy) microspheres showed retained superparamagnetism of the MSP core after the formation of the shell, although the saturation magnetization value decreased from 69.4 to 14.8 emu/g (Fig. 1h). Meanwhile, powder XRD results confirmed that the polymer shell didn't destroy the crystallinity of the MSP core (Fig. 1i). Compared to a previous report on fabrication of magnetic polymer composite microspheres,²⁸ our synthesis procedure didn't need modification of the magnetic core using silane coupling agents, such as γ -methacryloxypropyltrimethoxy (MPS), which can introduce an additional layer to complicate the particle degradation. Our successful encapsulation of MSP core by polymer shell was due to the direct interaction between the carboxylic acid group in MAA and the Fe ions in MSP.

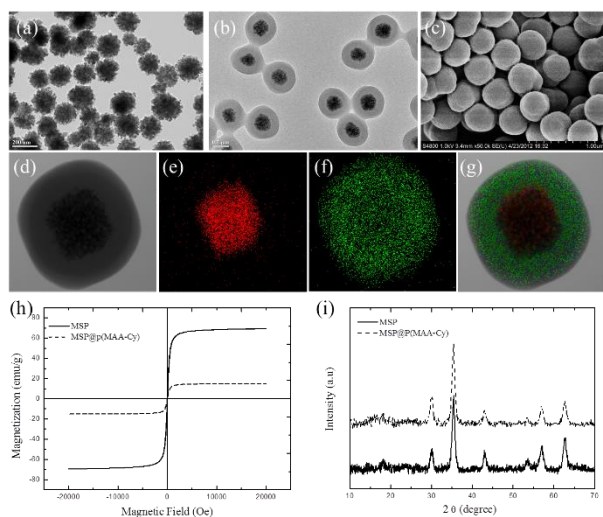


Fig. 1 (a) The TEM image of MSP; (b) TEM and (c) SEM images of MSP@P(MAA-Cy); The STEM images of EDX elemental mapping results: (d) the whole particles of MSP@P(MAA-Cy), (e) the Fe element distribution, (f) the S element distribution and (g) the merge image; (h) The VSM and (i) the XRD curves of MSP and MSP@P(MAA-Cy), respectively.

To investigate the effect of cross-linker Cy amounts on the formation of the polymer shell, DLS was applied to measure the size of the MSP@P(MAA-Cy) microspheres (Table 1). With the total amount of MAA and Cy at constant, increasing the fraction of Cy in the feed from 10 to 40 wt % increased the hydrodynamic diameter of the MSP@P(MAA-Cy) from 361 nm to 800 nm, which is in agreement to a literature report on the synthesis of P(MAA-Cy) nanogels.³⁰ Within our investigation, an optimized formulation of 30 wt% of Cy was used during the shell formation to produce the MSP@P(MAA-Cy) microspheres with the lowest polydispersity index (PDI) for further drug loading and release studies.

TABLE 1 The characterization data of MSP@P(MAA-Cy) with different cross-linker amounts.

Sample	Feeding fraction of Cy (wt%)	Size (nm)	PDI
MSP	/	153	0.137
MSP@P(MAA-Cy)-10	10	361	0.392
MSP@P(MAA-Cy)-20	20	585	0.154
MSP@P(MAA-Cy)-30	30	704	0.007

MSP@P(MAA-Cy)-40	40	808	0.028
------------------	----	-----	-------

Redox/pH-triggered degradation of MSP@P(MAA-Cy)

The shell and the core of the MSP@P(MAA-Cy) microspheres are sensitive to degradation when exposed to GSH-rich environment and acidic medium, respectively. According to the different intracellular environments between the tumor cells and normal cells,^{27,28} we chose two pH conditions (pH = 5.0 and 7.4) and two GSH concentrations (0 mM and 20 mM) to investigate the degradation of the MSP@P(MAA-Cy) microspheres by monitoring the turbidity of the particle dispersions (Fig. 2a). Without GSH, the disulfide bond in MSP@P(MAA-Cy) was intact and the relative transmissivity of the dispersion showed no change with time (Fig. 2a). In contrast, the relative transmissivity of the particle dispersion after addition of 20 mM GSH increased gradually and leveled off at 12 hours, indicating a complete degradation of the disulfide bonds. After 15-hour incubation, the relative transmissivity of sample continually increased in pH=5.0 but remained in pH=7.4, which was ascribed to the dissolution of the MSP core in acidic medium. Meanwhile, inductively coupled plasma (ICP) measurements detected an increased concentration of Fe ions in the supernatants after 15-hour incubation in a pH=5.0 buffer and confirmed the degradation of the MSP under acidic condition (Fig. 2b). In contrast, no Fe ion was detected in the supernatant of the pH=7.4 dispersion. In parallel studies, directly dispersing the core/shell MSP@P(MAA-Cy) particles in pH=5.0 buffer couldn't dissolve the MSP core and generated little detected Fe ions, probably due to the blocking of the diffusion of H⁺ through the cross-linked shell to the core. Thus, the degradation of the P(MAA-Cy) shell and the MSP core should be in order that the degradation of the shell exposed the MSP core to environment for further dissolution under acidic environment.

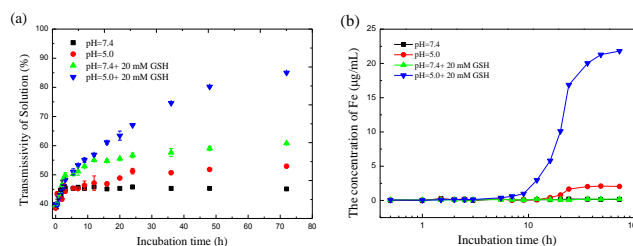


Fig. 2 (a) Transmissivity and (b) Fe element concentration in the supernatant of MSP@P(MAA-Cy) dispersion (0.2 mg/mL) in four types of buffer with different incubation time.

Two types of cells, HeLa cells (GSH-rich and acidic cytoplasm) and HEK 293T cells (GSH-lack and neutral cytoplasm),^{27,28} were employed to investigate the cell uptake of the MSP@P(MAA-Cy) microspheres and their degradation in cytoplasm. To track the polymer shell of particles in cells during degradation, rhodamine probe was covalently bound to the polymer shell based on amide reaction between the carboxylic acid group in PMAA and the amine group in rhodamine. In the first 3 hours, the rhodamine fluorescence in both cells could be detected and was limited in discrete spots instead of staining the whole cytoplasm, indicating no polymer degradation and release of rhodamine (Fig. 3a-3d). After 6 hours, the rhodamine fluorescence in HeLa cells started spreading to the whole cell and completely covered the cytoplasm at 24 hours (Fig. 3g-3i). In contrast, the rhodamine fluorescence in the HEK 293T cells remained on the particles instead of staining the whole cell upon to 24 hours (Fig. 3e-3j), demonstrating that the higher concentration of GSH in HeLa cells resulted in faster disassembly of P(MAA-Cy) shells in HeLa cells.

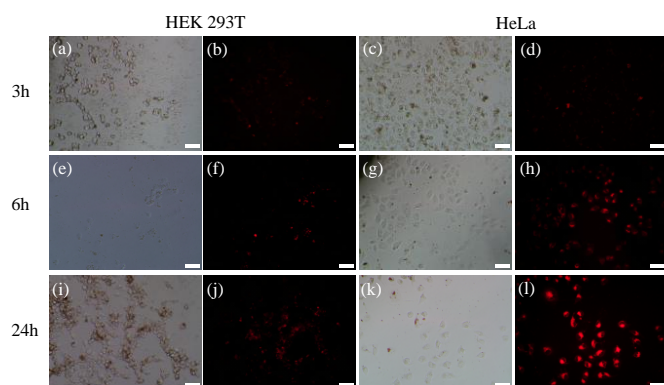


Fig. 3 The bright field and fluorescence microscope images of rhodamine grafted MSP@P(MAA-Cy) incubated with HEK 293T cells in (a, b) 3 hours, (e, f) 6 hours and (i, j) 24 hours and with HeLa cells in (c, d) 3 hours, (g, h) 6 hours and (k, l) 24 hours. The excitation wavelength for the fluorescence is 520 nm. All the scale bars are 40 μm .

To explore the degradation behavior of the MSP core in the cells, a Fe^{3+} -sensitive fluorescence probe (FP-1) was applied⁴¹ to monitor the variation of Fe^{3+} concentrations in the cytoplasm (Fig. 4). Red fluorescence was detected in HeLa cells after 24-hour incubation and became stronger at 48 hours. In contrast, no red fluorescence was detected in the cytoplasm of HEK 293T cells after incubation with MSP@P(MAA-Cy) for 48 hours, demonstrating the selective dissolution of MSP only in HeLa cell cytoplasm. These results, combining with the previous degradation studies of the polymer shells in these two cells, suggested that HeLa cells have a cytoplasm with higher GSH concentration and lower pH value than that of HEK 293T cells, which can rapidly and sequentially degrade the MSP@P(MAA-Cy) microspheres with a GSH-sensitive shell and an acid-sensitive core.

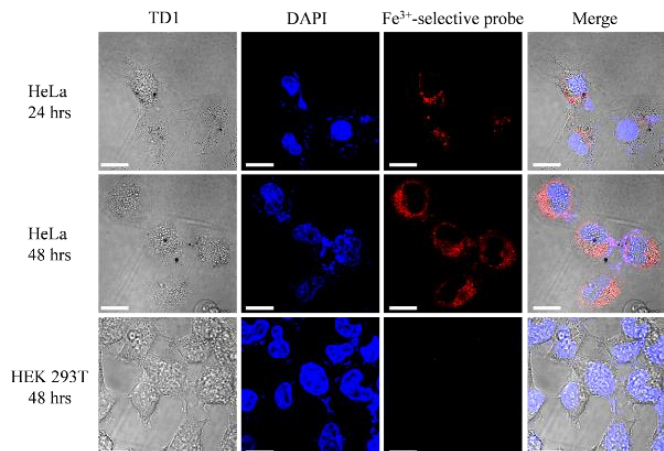


Fig. 4 The confocal laser scanning microscope (CLSM) images of the HeLa cells and HEK 293T cells incubated with FP-1-loaded MSP@P(MAA-Cy) in 24 hours or 48 hours. The DAPI can stain cell nucleus to blue and Fe^{3+} -selective probe can combine with Fe^{3+} in cells to show red fluorescence. All the bars are 10 μm .

Tailoring the controlled release of drugs from MSP@P(MAA-Cy)

Both the core and the shell in a MSP@P(MAA-Cy) can be used to store guest molecules, and its low cytotoxicity have been evidenced by our previous report,³¹ which is fit for guest molecules delivery in biomedicine. In addition, the protection of the polymer shell around the MSP core can provide an additional tool to tune the dissolution of the core and the release of the encapsulated molecules. In this study, FITC was used as a model guest molecule to be covalently

grafted into the mesoporous MSP core (MSP-FITC) before the deposition of the cross-linked polymer shell with loaded rhodamine dye, producing a fluorescent dye-labeled multifunctional microsphere (MSP-FITC@P(MAA-Cy)-Rho). The MSP-FITC@P(MAA-Cy)-Rho was incubated with HeLa cells and HEK 293T cells respectively, and the release behaviors of these two dyes were monitored using the CLSM (Fig. 5). Since the rhodamine interacts with PMAA shell by electrostatic interaction, it was easily released into the cytoplasm of both cells and stained the entire cytoplasm to red after 48 hours. In contrast, FITC was only released in HeLa cells, not in HEK 293T cells, since the high concentration of GSH in HeLa cells degraded the Cy cross-linked polymer shell and exposed the MSP core to the more acidic cytoplasm for degradation and release of FITC. Based on these results, the MSP@P(MAA-Cy) microspheres can be used to encapsulate different guest molecules in different position (shell and core) respectively and can selectively release core-loaded molecules in different cells.

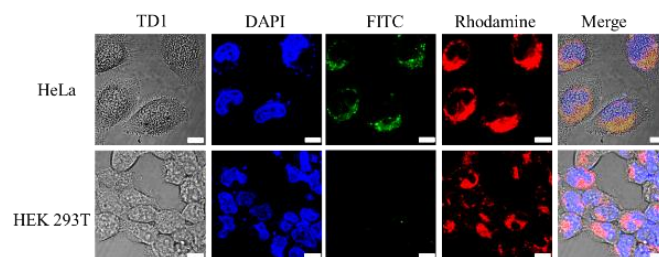


Fig. 5 The confocal laser scanning microscope (CLSM) images of HeLa cells and HEK 293T cells incubated with MSP-FITC@P(MAA-Cy)-Rho for 48 hours. All the bars are 5 μm .

In this section, anti-cancer drug DOX was loaded in the polymer shell based on electrostatic interaction with a loading amount of 31.8 wt % measured by UV-vis spectroscopy.³⁰ Considering the dual sensitivity of the microspheres to GSH and pH, four conditions were selected to investigate the release of DOX from MSP@P(MAA-Cy)-DOX microspheres (Fig. 6). At high GSH concentration (10 mM) and low pH=5.0, DOX can quickly release from the GSH-sensitive polymer shell due to the cleavage of disulfide bond and the protonation of the carboxylic acid groups to break up the electrostatic interaction.³⁰

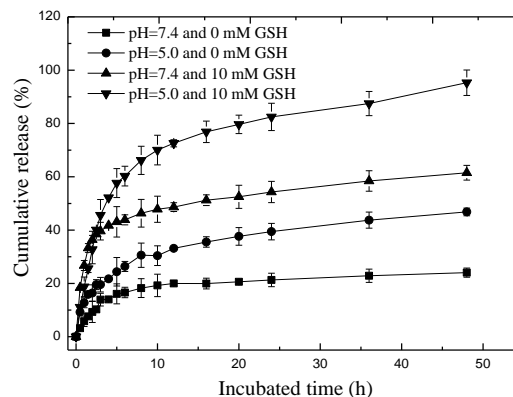


Fig. 6 Drug release profile of DOX from the MSP@P(MAA-Cy)-DOX with different pH values at 37 °C in different buffer.

In another synthesis, an anti-cancer drug TXL was loaded into the porous MSP core (MSP-TXL) before coating with a polymer shell to form a MSP-TXL@P(MAA-Cy) core/shell microsphere with an

overall TXL loading rate around 4.1 wt %. To investigate the tumor inhibitory effect, both MSP-TXL and MSP-TXL@P(MAA-Cy) were incubated with the HeLa cells and the HEK 293T cells before the measurement of the in vitro cytotoxicity using the CCK-8 method (Fig. 7). Since the MSP could be dissolved in the cytoplasm of HeLa cells, the MSP-TXL exhibited significant cytotoxicity after 48 hours, confirming the release of TXL to the cytoplasm of HeLa cells (Fig. 7a). In contrast, the MSP-TXL showed little cytotoxicity to the HEK 293T cells even at high concentrations (Fig. 7b). When MSP-TXL@P(MAA-Cy) particles were incubated with the cells, significant toxicity was detected in HeLa cells after 72 hours (Fig. 7c), longer than 48 hours because the degradation of the polymer shell took time before the exposure of the MSP cores to dissolution. Again, no cytotoxicity was determined in HEK 293T cells at all concentrations and any incubation time, (Fig. 7d), indicating little decomposition of the MSP-TXL@P(MAA-Cy) microsphere in HEK 293T cells. The controlled release property of TXL from the MSP-TXL@P(MAA-Cy) is highly important not only to retain a good inhibitive effect for cancer cells but also protect normal cells from side-effect of TXL.

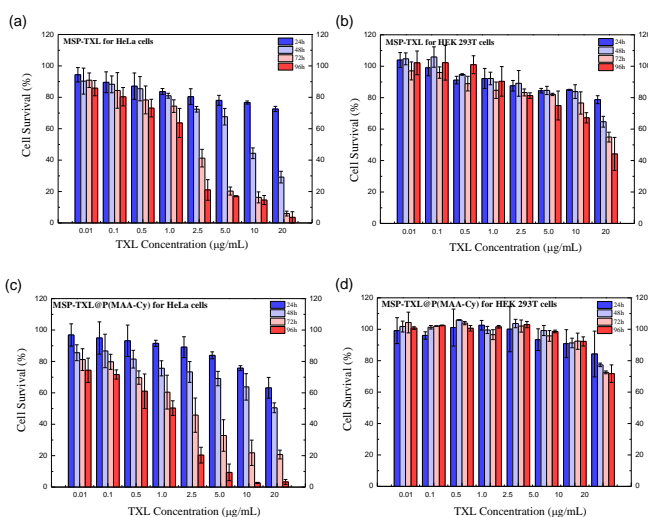


Fig. 7 The cell survival of (a) HeLa cells and (b) HEK 293T cells at different concentrations of the MSP-TXL, (c) HeLa cells and (d) HEK 293T cells at different concentrations of the MSP-TXL@P(MAA-Cy) after incubation for 24 hours, 48 hours, 72 hours and 96 hours, respectively.

In a further step when loading both drugs in the MSP core and the P(MAA-Cy) shell, respectively, the produced MSP-TXL@P(MAA-Cy)-DOX was evaluated on its toxicity using HeLa cells. As comparison, free DOX, free drug mixture of DOX and TXL (DOX:TXL=10:1), and the MSP@P(MAA-Cy)-DOX (without TXL loaded in core) were applied as controls. Both MSP@P(MAA-Cy)-DOX and MSP-TXL@P(MAA-Cy)-DOX showed higher cytotoxicity than free DOX and free DOX+TXL within 24 hours, which could be attributed to the quick cell uptake of the microspheres (Fig. 8a). Meanwhile, the MSP-TXL@P(MAA-Cy)-DOX showed higher cytotoxicity to HeLa cells than the MSP@P(MAA-Cy)-DOX after 48-hour incubation (Fig. 8b) because of the release of two drugs from the MSP-TXL@P(MAA-Cy)-DOX. In this case, the TXL in MSP-TXL@P(MAA-Cy)-DOX could be released, following with the complete degradation of shell to release the DOX. While the DOX entered nucleus and intercalated the DNA of HeLa cells,⁴² the TXL gradually released to interact with other organelles such as microtubule, assisting DOX to damage the cancer cells.⁴⁰ This synergistic effect reinforced the inhibiting ability, which demonstrated its great potential for cancer therapy.

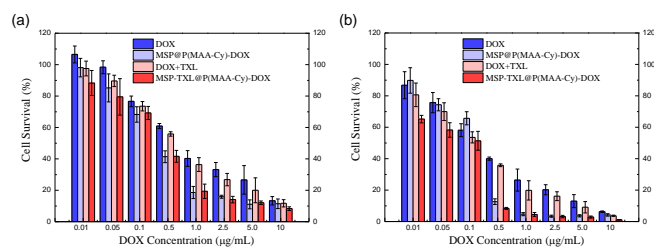


Fig. 8 The cell survival of HeLa cells at different concentrations of free DOX, free drug mixture of DOX and TXL (DOX+TXL), MSP@P(MAA-Cy)-DOX, and MSP-TXL@P(MAA-Cy)-DOX after incubation with HeLa cells for (a) 24 hours and (b) 48 hours, respectively.

Conclusions

In summary, we designed a novel biodegradable core/shell-structured MSP@P(MAA-Cy) microsphere that contained an acid-dissolvable MSP core and a redox-degradable polymer shell. The shell and the core could be sequentially and completely degraded under both simulated physiological conditions (10 mM GSH and pH=5) and HeLa cellular environment. Two anticancer drugs, TXL and DOX, were successfully loaded into the core and the shell of the composite microspheres with high loading rates to produce a novel multi-functional drug delivery system (MSP-TXL@P(MAA-Cy)-DOX) that carried the two drugs in different domains. Experimental results proved that the drugs could be sequentially released responding to different stimuli, and the dual-drug carrier exhibited much better inhibition effect for HeLa cells' propagation than free DOX, free dual-drugs (DOX+TXL) and single-drug loaded composite microspheres. Through the assistance of external magnetization, these MSP@P(MAA-Cy) microspheres should have great potential to be used in targeting drug delivery system to achieve programmed drug release characteristics.

Acknowledgements

This work was supported by National Science and Technology Key Project of China (Grant No. 2012AA020204); Science and Technology Commission of Shanghai (Grant Nos. 13JC1400500 and 13520720200). H.G. also thanks the University of Notre Dame, the Center for Sustainable Energy at Notre Dame (cSEND), and the Senior Visiting Scholar Foundation of Key Laboratory in Fudan University, China for financial support.

Notes and references

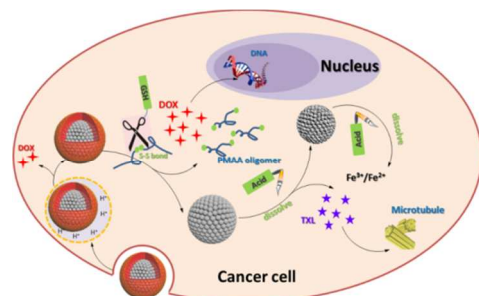
- ^a State Key Laboratory of Molecular Engineering of Polymers, Department of Macromolecular Science, and Laboratory of Advanced Materials, Fudan University, Shanghai, 200433, People's Republic of China; E-mail: ccwang@fudan.edu.cn; Fax: +86-21-65640293; Tel: +86-21-65642385.
- ^b Department of Chemistry and Biochemistry, 251 Nieuwland Science Hall, University of Notre Dame, Indiana 46556-5670, USA.

- 1 T. M. Allen, P. R. Cullis, *Science*, 2004, **303**, 1818-1822.
- 2 D. Peer, J. M. Karp, S. Hong, O. C. Farokhzad, R. Margalit, R. Langer, *Nat. Nanotechnol.*, 2007, **2**, 751-760.

3. F. Danhier, O. Feron, V. Pr at, *J. Control. Release*, 2010, **148**, 135-146.
4. C. R. Thomas, D. P. Ferris, J. H. Lee, E. Choi, M. H. Cho, E. S. Kim, *J. Am. Chem. Soc.*, 2010, **132**, 10623-10625.
5. S. Brul  M. Levy, C. Wilhelm, D. Letourneur, F. Gazeau, C. M nager, C. Le Visage, *Adv. Mater.*, 2011, **8**, 787-790.
6. T. J. Yoon, J. S. Kim, B. G. Kim, K. N. Yu, M. H. Cho, J. K. Lee, *Angew. Chem. Int. Ed.*, 2005, **44**, 1068-1071.
7. E. Ruiz-Hernandez, A. Baeza, M. Vallet-Regi, *ACS Nano*, 2011, **5**, 1259-1266.
8. S. Peng, S. H. Sun, *Angew. Chem. Int. Ed.*, 2007, **46**, 4155-4158.
9. S. H. Liu, R. M. Xing, F. Lu, R. K. Rana, J. J. Zhu, *J. Phys. Chem. C*, 2009, **113**, 21042-21047.
10. K. Cheng, S. Peng, C. J. Xu, S. H. Sun, *J. Am. Chem. Soc.*, 2009, **131**, 10637-10644.
11. J. Liu, Z. K. Sun, Y. H. Deng, Y. Zou, C. Y. Li, X. H. Guo, L. Q. Xiong, Y. Gao, F. Y. Li, D. Y. Zhao, *Angew. Chem. Int. Ed.*, 2009, **48**, 5875-5879.
12. B. Luo, S. Xu, W. F. Ma, W. R. Wang, S. L. Wang, J. Guo, W. L. Yang, J. H. Hu, C. C. Wang, *J. Mater. Chem.*, 2010, **20**, 7107-7113.
13. S. Xu, B. R. Yin, J. Guo, C. C. J. *Mater. Chem. B*, 2013, **1**, 4079-4087.
14. B. Luo, S. Xu, A. Luo, W. R. Wang, S. L. Wang, J. Guo, Y. Lin, D. Y. Zhao, C. C. Wang, *ACS Nano*, 2011, **5**, 1428-1435.
15. S. Xu, C. Sun, J. Guo, K. Xu, C. C. Wang, *J. Mater. Chem.*, 2012, **22**, 19067-19075.
16. J. Panyam, V. Labhasetwar, *Adv. Drug Delivery Rev.*, 2003, **55**, 329-347.
17. G. B. Sukhorukov, A. L. Rogach, M. Garstka, S. Springer, W. J. Parak, A. Munoz-Javier, O. Kreft, A. G. Skirtach, A. S. Susha, Y. Ramaye, R. Palankar, M. Winterhalter, *Small*, 2007, **3**, 944-955.
18. C. Kim, S.S. Agasti, Z. Zhu, L. Lsaacs, V. M. Rottello, *Nat. Chem.*, 2010, **2**, 962-966.
19. A. L. Becker, N. I. Orlotti, M. Folini, F. Cavalieri, A. N. Zelikin, A. P. R. Johnston, N. Zaffaroni, F. Caruso, *ACS Nano*, 2011, **5**, 1335-1344.
20. Y. Yan, A. P. R. Johnston, S. J. Dodds, M. M. J. Kamphuis, C. Ferguson, R. G. Parton, E. C. Nice, J. K. Heath, F. Caruso, *ACS Nano*, 2010, **4**, 2928-2936.
21. H. Meng, M. Xue, T. Xia, Y. L. Zhao, F. J. Tamanoi, F. Stoddart, J. I. Zink, A. E. Nel, *J. Am. Chem. Soc.*, 2010, **132**, 12690-12697.
22. S. Aryal, C. M. J. Hu, L. F. Zhang, *ACS Nano*, 2010, **4**, 251-258.
23. C. Park, H. Kim, S. Kim, C. Kim, *J. Am. Chem. Soc.*, 2009, **131**, 16614-16615.
24. R. Tang, C. S. Kim, David J. Solfiell, S. Rana, R. Mout, E. M. Vel quez-Delgado, A. Chompoosor, Y. Jeong, B. Yan, Z. J. Zhu, C. Kim, J. A. Hardy, Vincent M. Rotello, *ACS Nano*, 2013, **7**, 6667-6673.
25. C. Park, K. Lee, C. Kim, *Angew. Chem. Int. Ed.*, 2009, **48**, 1275-1278.
26. J. H. Lee, K. J. Chen, S. Hyun. Noh, M. A. Garcia, H. Wang, W. Y. Lin, H. Jeong, B. J. Kong, David B. Stout, J. Cheon, H. R. Tseng, *Angew. Chem. Int. Ed.*, 2013, **52**, 4384-4388.
27. S. M. Simon, *Drug Discovery Today*, 1999, **4**, 32-38.
28. R. Hong, G. Han, J. M. Fernandez, B. J. Kim, N. S. Forbes, V. M. Rotello, *J. Am. Chem. Soc.*, 2006, **128**, 1078-1079.
29. Q. Zhang, F. Liu, K. Truc Nguyen, X. Ma, X. J. Wang, B. G. Xing, Y. L. Zhao, *Adv. Funct. Mater.*, 2012, **22**, 5144-5156.
30. Y. J. Pan, Y. Y. Chen, D. R. Wang, C. Wei, J. Guo, D. R. Lu, C. C. Chu, C. C. Wang, *Biomaterials*, 2012, **33**, 6570-6579.
31. W. F. Ma, K. Y. Wu, J. Tang, D. Li C. Wei, J. Guo, S. L. Wang, C. C. Wang, *J. Mater. Chem.*, 2012, **22**, 15206-15214.
32. D. Li, Y. T. Zhang, M. Yu, G. Jia, D. Chaudhary, C. C. Wang, *Biomaterials*, 2013, **34**, 7913-7922.
33. K. Barick, S. Singh, Neena V. Jadhav, D. Bahadur, B. Pandey, P. Hassan, *Adv. Funct. Mater.*, 2012, **22**, 4975-4984.
34. D. Li, J. Tang, C. Wei, J. Guo, S. L. Wang, D. Chaudhary, C. C. Wang, *Small*, 2012, **8**, 2690-2698.
35. D. Li, J. Tang, J. Guo, S. L. Wang, D. Chaudhary, C. C. Wang, *Chem. Eur. J.*, 2012, **18**, 16517-16524.
36. Z. Luo, K. Y. Cai, Y. Hu, J. H. Li, X. W. Ding, B. L. Zhang, D. W. Xu, W. H. Yang, P. Liu, *Adv. Mater.*, 2012, **24**, 431-435.
37. H. Meng, W. X. Mai, H. Y. Zhang, M. Xue, T. Xia, S. J. Lin, X. Wang, Y. Zhao, Z. X. Ji, J. I. Zink, A. E. Nel, *ACS Nano*, 2013, **7**, 994-1005.
38. P. M. Valencia, E. M. Pridgen, B. Perea, S. Gadde, C. Sweeney, P. W. Kantoff, N. H. Bander, S. J. Lippard, R. Langer, R. Karnik, O. C. Farokhzad, *Nanomedicine*, 2013, **8**, 687-698.
39. T. Thambi, V. G. Deepagan, H. Ko, D. S. Lee, J. H. Park, *J. Mater. Chem.*, 2012, **22**, 22028-22036.
40. Y. D. Gu, Y. N. Zhong, F. H. Meng, R. Cheng, C. Deng, Z. Y. Zhong, *Biomacromolecules*, 2013, **14**, 2772-2780.
41. M. Zhang, Y. H. Gao, M. Y. Li, M. X. Yu, F. Y. Li, L. Li, *Tetrahedron Lett.*, 2007, **48**, 3709-3712.
42. C. C. Wu, D. Han, T. Chen, L. Peng, G. Z. Zhu, M. X. You, L. P. Qiu, K. Sefah, X. B. Zhang, W. H. Tan, *J. Am. Chem. Soc.*, 2013, **135**, 18644-18650.

ARTICLE

Table of Contents



Redox/pH dual-stimuli-responsive drug delivery system for programmed release of anticancer drugs has been developed for enhancing the therapeutic effect.